Supporting Information

Effective Charge Separation of Inverted Polymer Solar Cells using Versatile MoS_2 Nanosheets as Electron Transport Layer

Kyu Seung Lee[a,||], Young Jae Park[a,||], Jaeho Shim[a,b], Chil-Hyoung Lee[a], Guh-Hwan Lim[a], Hak Yong Kim[c,d], Jin Woo Choi[e], Chang-Lyoul Lee[e], Yeonghoon Jin[b], Kyoungsik Yu[b], Hee-Suk Chung[f], Basavaraj Angadi[g], Seok-In Na[h], and Dong Ick Son[a,i*]

[a]Institute of Advanced Composite Materials, Korea Institute of Science and Technology, 92 Chudong-ro, Bongdong-eup, Wanju-gun, Jeonbuk, 55324, Republic of Korea

[b]School of Electrical Engineering, Korea Advanced Institute of Science and Technology, 291 Daehak-ro, Yuseong-gu, Daejeon 34141, Republic of Korea

[c]Department of BIN Convergence technology, Chonbuk National University, 567 baekje-daero, Deokjin-gu, Jeonju, Jeonbuk, 54896, Republic of Korea

[d]Department of Organic Materials & Fiber Engineering, Chonbuk National University, 567 Baekje-daero, Deokjin-gu, Jeonju, Jeonbuk, 54896, Republic of Korea

[e]Advanced Photonics Research Institute, Gwangju Institute of Science and Technology,1 Oryong-dong Buk-gu, Gwangju 500-712, Republic of Korea

[f]Analytical Research Division, Korea Basic Science Institute, 20 Geonji-ro, Deokjin-gu, Jeonju, Jeonbuk, 54907, Republic of Korea

[g]Department of Physics, Bangalore University, Bangalore, 560–056, India

[h]Professional Graduate School of Flexible and Printable Electronics and Polymer Materials Fusion Research Center, Chonbuk National University, Jeonju-si, Jeonbuk, 664-14, Republic of Korea

---

*Corresponding author: *E-mail address*: eastwing33@kist.re.kr (D. I. Son) Tel: +82 63 2198155, Fax: +82 63 2198129

|| These authors contributed equally to this work.

† Electronic supplementary information (ESI) available: additional topographic images, and additional ADF and ABF images, and additional UPS data of PEIE/ITO/glass, and additional energy band diagram.

[i]KIST school, Department of Nanomaterials and Nano Science, University of Science and Technology (UST), Daejeon 34113, Republic of Korea

Contents

1. Experimental

1. 1. Exfoliation of MoS_2 Nanosheets: 2 g of the commercial MoS_2 sheets (2D semiconductor) was dispersed in 1 L of ethanol. The MoS_2 dispersion was treated by tip-sonication for 5 hours. Then, the MoS_2 dispersion was centrifuged for 30 min at 8000 rpm to collect a supernatant and remove precipitation. The initial concentration of the MoS_2 NS supernatant was 100 ± 2.7 mg/L. Then, the supernatant was diluted in 1mL of ethanol and the concentration was estimated to be about 16.67 mg/L.

1. 2. Characterization of MoS_2 Nanosheets: The MoS_2 NSs were characterized through TEM, AFM, Raman spectroscopy, UV-vis absorption spectroscopy, and PL spectroscopy. The TEM images were obtained using a Philips Tecnai G2 F20 TEM microscope with an accelerating voltage of 200 kV. The AFM surface images and height distribution were measured by Park system NX10. The MoS_2 NSs solution in DMF was deposited on a silicon wafer by spin coating and drying under ambient conditions. The AFM image was obtained in a tapping mode. Different concentrations of MoS_2 NSs solution were used to achieve layers deposited on SiO_2/Si substrate. Raman spectra of MoS_2 NSs were obtained using a Horiba Jobin Yvon-Labram HR UV visible NIR Raman microscope spectrometer with a 514 nm Ar laser. Ultraviolet-visible (UV-vis) absorption spectra of the MoS_2 NSs measured with a Shimadzu, UV-2600 UV-vis spectrophotometer. PL spectra were obtained using a Horiba NanoLog-C. To demonstrated the MoS_2 NSs of energy levels using electrochemical cyclic voltammetry. MoS_2 NSs were dispersed in a 0.5% Nafion solution (isopropanol and dimethylformamide) and dropped on glassy carbon electrode to serve as the working electrode. The counter electrode and the reference electrode were platinum wire and $Ag/AgNO_3$ (in 0.01 M MeCN), respectively, and the electrolyte was a solution of 0.1 M tetrabutylammonium phosphorus hexa fluoride (TBAPF6) in anhydrous acetonitrile. Measurements were performed at room temperature with a scan rate of 100 mV/s.

1. 3. Device fabrication process of iPSCs: 1.5 × 1.5 cm^2 patterned ITO-coated glass substrates were cleaned with acetone, ethanol, and 2-propanol, respectively. The ITO-coated glass was treated with O_2 plasma for 40 sec. PEIE layer was spin-coated on the ITO-coated glass at 4000 rpm for 40 sec, and the substrate was annealed at 110 °C for 10 min. After annealing, 0.1 ml of MoS_2 NSs in 1 ml of ethanol solution was spin-coated on the PEIE surface at 4000 rpm for 40 sec, followed by annealing at 140 °C for 10 min under ambient conditions. The substrates were transferred into a nitrogen-filled glove box. The blend of P3HT:PC_{60}BM (1.5:1 (by weight)), PTB7:PC_{71}BM (1:1.5 (by weight)), PTB7-Th:PC_{71}BM (1:1.5 (by weight)) solution were spin-coated onto the MoS_2 NSs interlayer at 2000 rpm for 10 sec and 1400 rpm for 10 sec, respectively. Finally, MoO_3 (10 nm) and Ag (80 nm) were deposited by thermal evaporation on the active layer under a pressure of $1x10^{-6}$ Torr.

1. 4. Characterization of iPSCs structures: The structures of iPSCs with the MoS_2 NSs/PEIE/ITO/glass were characterized through Focused Ion Beam (FIB), TEM and STEM-EDS. In detail, The FIB was applied for cross-sectional sample preparation of iPSCs with both TEM and STEM-EDS. Thinly sliced TEM samples were prepared using a FIB (Nova nanolab 600 Dual Beam) operating at 5~20 kV with Ga ions. The TEM images were obtained using a Philips Tecnai G2 F20 TEM microscope with an accelerating voltage of 200 kV. The STEM-EDS images were obtained using a JEM-ARM200F Cs-corrected STEM.

1. 5. Photovoltaic device characterization of iPSCs with/without MoS_2 Nanosheets: The iPSCs were then tested in air under an AM 1.5 G illumination of 100 mW/cm^2 (Oriel 1 kW solar simulator), which was calibrated with the International System of Units (SI) (SRC-1000-TC-KG5-N, VLSI Standards, Inc) for accurate measurement. The external quantum efficiency (EQE) was measured using an Oriel IQE-200 (Newport), a calibrated Si UV detector and an SR8570 low noise current amplifier. In TCSPC, photo-excitation was carried out by the mode-locked titanium: sapphire laser with the wavelength of 400 nm and luminescence signals were detected by an InGaAs based photomultiplier detector.

2. The topographic images of MoS_2 NSs and line profile.

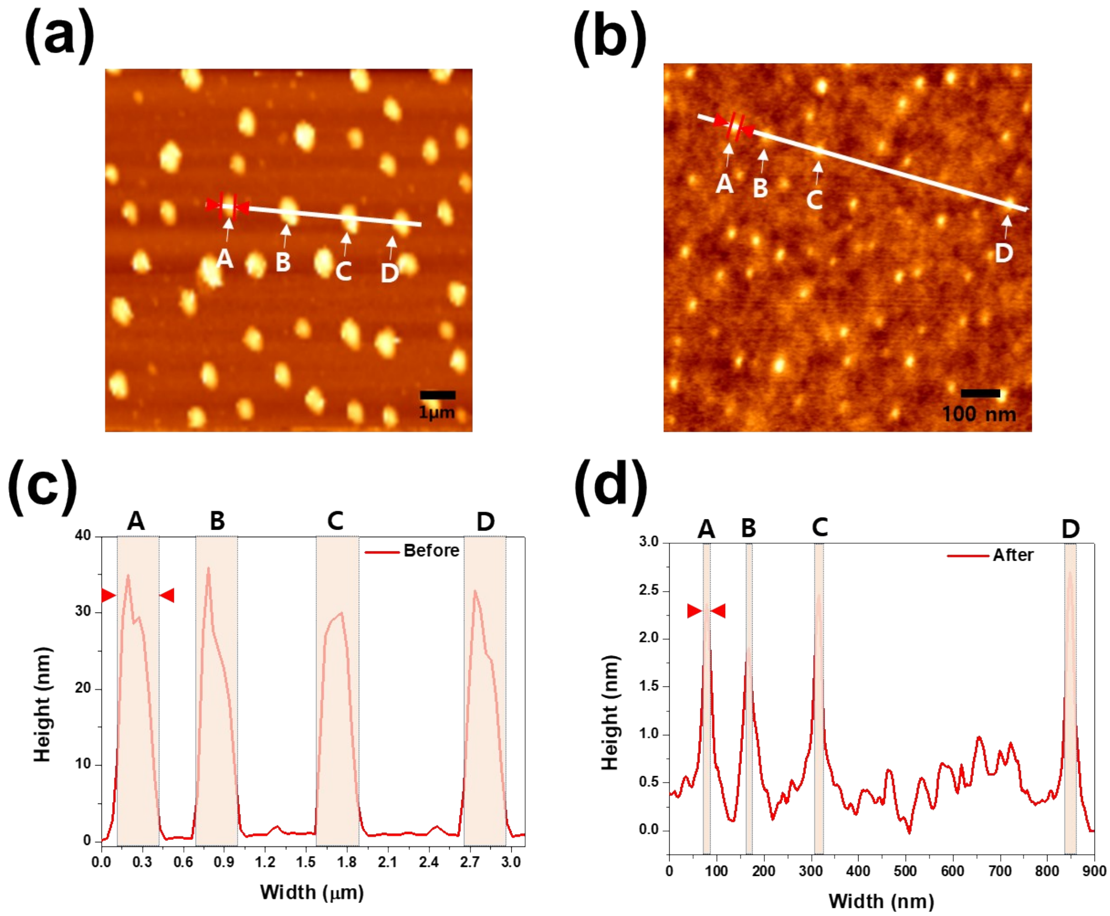

Figure S1. Topographic images and line profiles of the MoS_2 NSs before (a) and (c) after tip-sonication exfoliation and centrifugation process (b) and (d) corresponding to the white line in the topographic images.

3. The topographic images of SiO_2 on Si substrate and PEIE on SiO_2 on Si substrate.

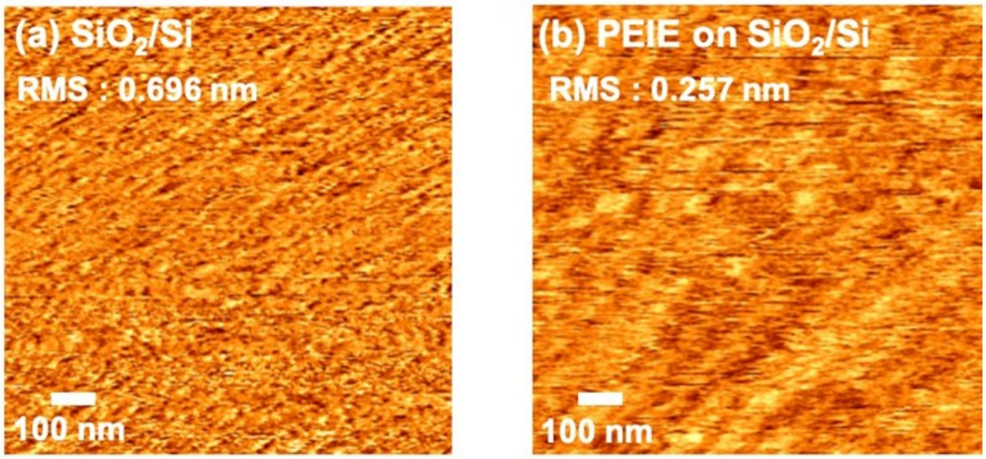

Figure S2. Topographic images RMS values of the SiO_2 on Si (a) and PEIE on SiO_2 on Si substrate (b).

4. The annular dark field (ADF) and annular bright field (ABF) images of the MoS_2 NSs on the PEIE/ITO/glass.

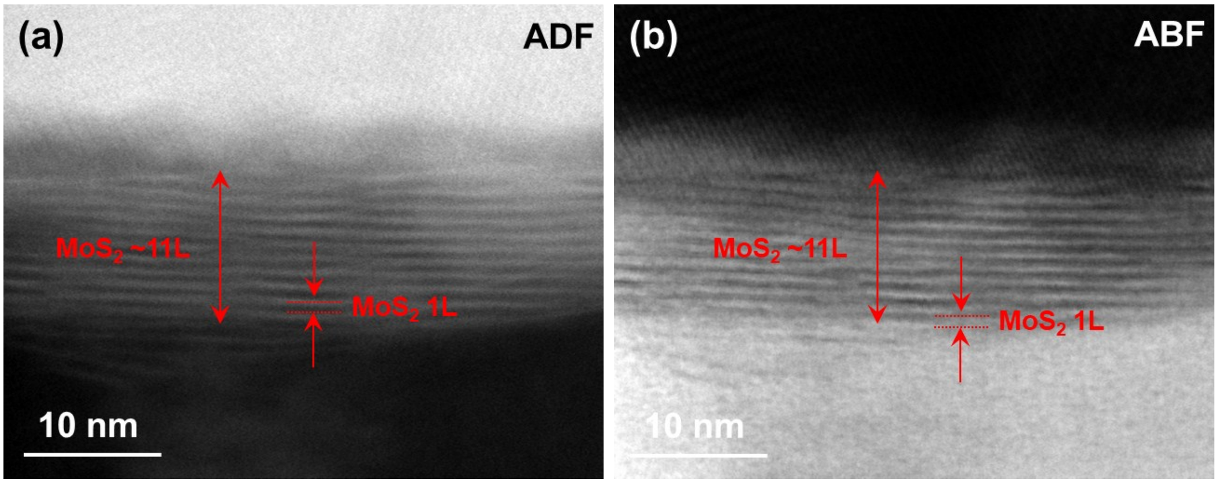

Figure S3. The annular dark field (ADF) and annular bright field (ABF) images of the MoS_2 NSs.

We performed image analysis of MoS_2 NSs by a spherical aberration-corrected scanning TEM (Cs-TEM). As shown in Fig. S2(a) and S2(b), we show the annular dark field (ADF) and annular bright field (ABF) images of the MoS_2 NSs and the ITO/glass substrate. Through the ADF and ABF images, the contrast of the MoS_2 NSs layer was improved by confirming the shape of the MoS_2 NSs. As a result, MoS_2 NSs applied as ETL could be clearly confirmed.

5. The work function (Φ) of the spin-coated PEIE onto ITO/glass and ITO/glass calculated by using an ultraviolet photoelectron spectroscopy (UPS).

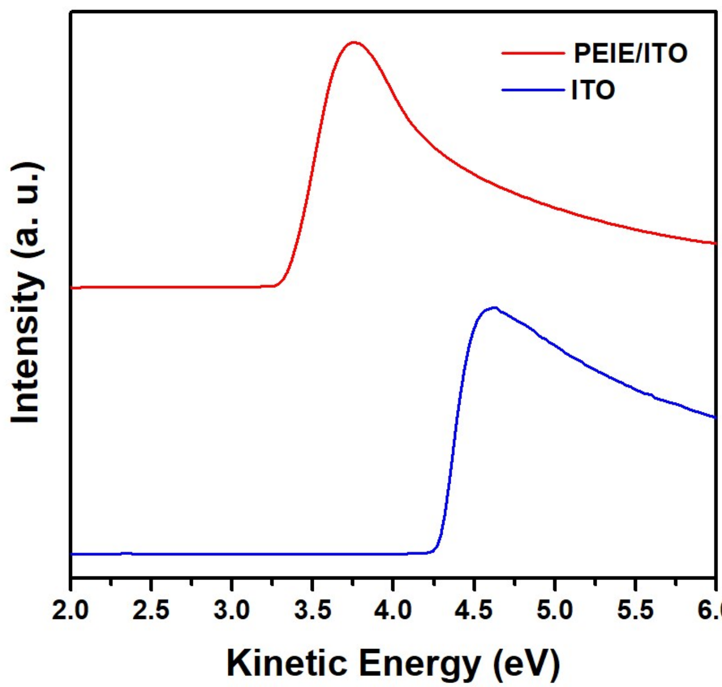

Figure S4. The work function of the PEIE/ITO/Glass and ITO/Glass.

The work function value of the ITO, PEIE/ITO structures obtained 4.29 eV, 3.36 eV, respectively. In this structure, the PEIE layer plays a role as a surface modifying layer on the ITO layer for good electron selectivity and efficiently promotes electron transportation to decrease the work function of ITO due to the formation of dipole layer.[1]

6. Energy level diagram of the iPSCs with the MoS_2 interlayer highlighting pathways for charge generation and transport.

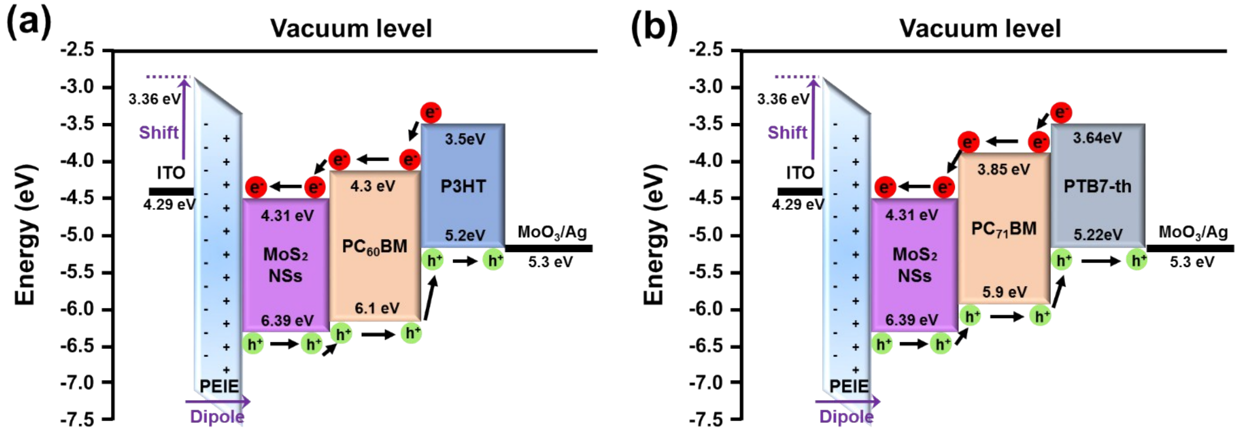

Figure S5. Energy level diagrams of the inverted PSCs with the MoS_2 interlayer.

The energy level diagrams of iPSCs demonstrate the possible pathways of current generation and transportation after the excitation of the photoactive materials P3HT:PC_{60}BM (a) and PTB7-th:PC_{71}BM (b).[2]

7. The structure of optical absorption simulation.

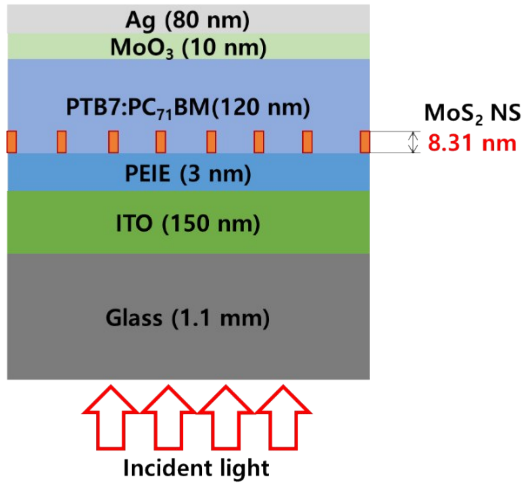

Figure S6. The structure of optical absorption simulation.

The solar cell structure used for the simulation is the Ag (80 nm)/MoO_3 (10 nm)/PTB7:$PC_{71}BM$ (120 nm)/MoS_2 (8.31 nm)/PEIE (3 nm)/ITO (150 nm)/glass (1.1 mm) structures. MoS_2 NS diameter: 25 nm and spacing between the edges of MoS_2 NS: 104 nm

Reference

(1) Hu, Z.; Wu, Z.; Han, Cheng.; He, J.; Ni, Z.; Chen, W. Two-dimensional transition metal dichalcogenides: interface and defect engineering. *Chem. Soc. Rev.* **2018,** *47,* 3100-3128.

(2) Chen, W.; Qi, D.; Gao, X.; Wee, A. T. S. Surface transfer doping of semiconductors. *Prog. Surf. Sci.* **2009,** *84,* 279-321.